Effect of heat release on the stability of compressible reacting mixing layer

By D. S. Shin AND J. H. Ferziger

1. Motivation and objectives

Reacting free shear layers are of fundamental importance in many industrial systems including gas turbine combustors and rockets. Efficient propulsion systems are essential for air breathing supersonic ramjets in the high Mach number range. A limiting factor in these engines is the time for fuel and oxidizer to mix in the combustion chamber; for fast mixing, the flow must be vigorously turbulent which requires the laminar flow to be unstable. Understanding the stability characteristics of compressible reacting free shear layers is, therefore, very important and may allow one to control the flow. Low speed shear layers are highly unstable but, as chemical reaction (Shin & Ferziger 1990) and compressibility effects (Brown & Roshko 1974; Papamoschou & Roshko 1988) tend to stabilize them, it is important to investigate the stability of high speed reacting mixing layers. The latter consists of two fluid streams containing fuel and oxidizer respectively, and the conclusions are expected to apply, with quantitative modifications, to other shear flows, e.g., jets. Since low speed reacting cases have been studied earlier (Shin & Ferziger 1990), we concentrate on the effects of Mach number and heat release.

We are primarily interested in solving the stability problem over a large range of Mach number and heat release. In order to understand the effect of the heat release on the stability of this flow, one must first study the characteristics of the non-reacting flow. Inviscid theory is a reliable guide for understanding stability of compressible shear flows at moderate and large Reynolds numbers and is the basis for this work.

2. Accomplishments

2.1 Laminar flow profiles

Since in our previous report (Shin & Ferziger 1990) we have shown the importance of using correct laminar profiles rather than assumed analytical ones, we began by computing such profiles. To generate mean profiles, we solved the (parabolic) compressible boundary-layer equations. Uniform pressure across the shear layer and unity Lewis and Prandtl numbers are assumed for simplicity. Prandtl number 0.7 does not produce large quantitative differences. We considered only the case in which the ratio of the speed of the slow stream to that of the fast stream is 0.5 to reduce the parameter range. The static temperature is initially uniform, and the mass fractions of free streams are specified. The inlet profiles are taken from self-similar solutions of the equations without heat release; their effect diminishes downstream.

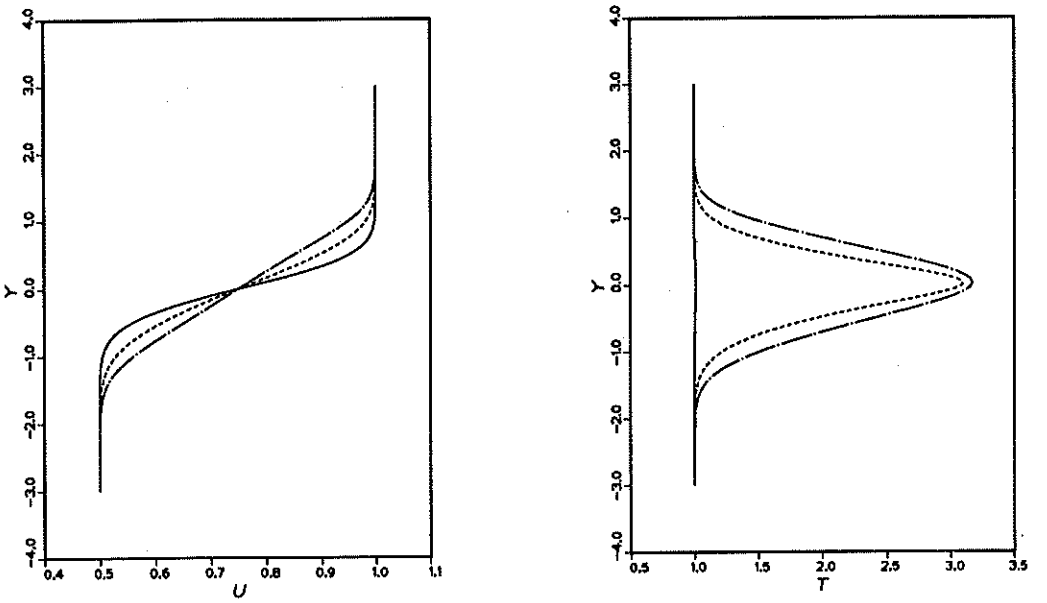

FIGURE 1. Effect of heat release and variable transport properties of the spatially developing layer at M_c=0.25 on the (a) velocity (b) temperature profiles. ——— , T_{ad}=1; ---- , T_{ad}=7 (constant property); —·— , T_{ad}=7 (variable property).

Variable transport properties and chemical reaction, which were shown to be important in low-speed flow, are included. For the transport properties, power laws in temperature and pressure are assumed:

$$\mu \propto P^0 T^{0.7} \; ; \quad \kappa \propto P^0 T^{0.7} \; ; \quad D \propto P^1 T^{1.7} \tag{1}$$

where μ is the viscosity, κ, the thermal diffusivity, and D, the mass diffusivity. Chemistry is treated by a single step irreversible scheme involving fuel and oxidizer reacting to yield product.

To satisfy the boundary-layer approximation, we used an initial Reynolds number of 1000 based on the initial vorticity thickness and cold viscosity. To include the coupling among the chemical reaction, heat release, and the velocity field, the conservation equations for the mass, energy, and species equations are solved simultaneously with the equation of state. As the compressible boundary-layer equations are parabolic, an implicit method (Crank-Nicolson) is used. Figure 1 compares the streamwise velocity and temperature profiles of spatial layers with the same inlet profiles and shows the effects of heat release and variable properties for a case with upper-stream Mach number M_1=1 and convective Mach number M_c=0.25. The non-dimensional adiabatic flame temperature T_{ad} is 7 for the reacting cases. These profiles are compared at a streamwise distance x normalized by the initial vorticity thickness of 57 downstream of the ignition point. The significant difference between the constant and variable property solutions indicates that property variations need

to be included whenever there are large temperature variations. Note that these flows have significantly different Reynolds numbers.

2.2 Inviscid linear stability equation

We assume that the laminar flow is parallel and subjected to small disturbances in the form of travelling waves. Each dimensionless quantity can be expressed as

$$F(x,y,z,t) = \overline{F}(y) + \hat{F}(y)e^{i(\alpha x+\beta z-\omega t)} \tag{2}$$

where $\overline{F}(y)$ is the laminar flow quantity, $\hat{F}(y)$ is eigenfunction depending only on the y coordinate, α, β are wavenumbers in the streamwise and spanwise directions respectively, and ω is the frequency. The relation between the wavenumbers and the angle of disturbance is

$$\tan\theta = \beta/\alpha. \tag{3}$$

For the temporal stability analysis, α is real and ω is complex, while for the spatial analysis, ω is real and α is complex. The corresponding amplification rates are ω_i and $-\alpha_i$. The perturbation equations are derived by linearizing the full compressible equations. Substituting (2) into these equations and neglecting the products of disturbances yields the disturbance equation for the pressure.

$$\hat{p}'' - \left\{\frac{2\alpha U'}{(\alpha U-\omega)} + \frac{R}{T}(\alpha U-\omega)^2[RXN1]\right\}\hat{p}' - q\hat{p} = 0$$

$$q = (\alpha^2+\beta^2) - \gamma {M_1}^2(\alpha U-\omega)^2\left\{\frac{1}{T} + \frac{R}{T}[RXN2]\right\} \tag{4}$$

where U, R and T are the laminar velocity, density and temperature respectively, and a prime denotes differentiation with respect to y. γ is the specific heat ratio and M_1 is the Mach number of the upper stream. $[RXN1]$ and $[RXN2]$ are terms which represent the effect of chemical reaction and associated heat release on the instability. The boundary conditions are obtained by considering the asymptotic form of the solutions of Equation (4). As $y \to \pm\infty$, U' and $[RXN1]$ become negligible and the solutions must behave like:

$$\hat{p}(y \to -\infty) = C_1 \exp(\sqrt{q}y)$$

$$\hat{p}(y \to \infty) = C_2 \exp(-\sqrt{q}y) \tag{5}$$

where C_1, C_2 are arbitrary constants, chosen as unity. An iterative method based on the shooting and Newton-Raphson methods are used to solve Equation (4). First, a guess of the eigenvalue is made. For a spatial analysis, ω is specified and α is guessed, whereas for temporal analysis, α is specified and ω guessed. Given the eigenvalue, we compute $\hat{p}$ for large y from Equation (5). Then we integrate Equation (4) from both free streams toward the centerline of the mixing layer, at y=0. At the centerline, the values of $\hat{p}$ and $\hat{p}'$ computed by integrating from the upper-stream, $\hat{p}_+(0)$ and $\hat{p}'_+(0)$, are compared with the values computed by integrating from the

lower-stream, $\hat{p}_-(0)$ and $\hat{p}'_-(0)$. If they match, the process has converged; if not, a new eigenvalue is chosen, and iteration continues until the eigenvalue converges to the specified tolerance. The integrations were carried out using subroutine ODE, and the update of the eigenvalue is based on the Newton-Raphson method. An error control of 10^{-6} was used for the integration, and iteration continued until the eigenvalue changed less than 10^{-7}. This method is applicable to both the temporal and spatial problems.

2.3 Multiple modes of instability

For compressible mixing layers, an inviscid neutral solution has a critical layer at a generalized inflection point where $(U'/T)'=0$. This is the necessary condition for neutral instability and is a generalization of the condition for low Mach number reacting flow (Shin & Ferziger 1990). We find that non-reacting incompressible flow has a single inflection point, whereas reacting or highly compressible flows have three.

We calculated the growth rates of the unstable modes. Figure 2 gives the maximum with respect to wavenumber of the amplification rate of two-dimensional modes as a function of the convective Mach number for $T_{ad}=1$ and 4 in the temporal layer. First consider the unheated flow ($T_{ad}=1$). As has been demonstrated by Groppengiesser (1970) and others (Blumen *et al.* 1975; Sandham & Reynolds 1989), the growth rate of the center mode decreases dramatically as the Mach number increases. In the highly supersonic regime, the growth rate is miniscule compared to its incompressible value. At supersonic speeds, a second set of modes, which we shall call the outer modes, become unstable. The growth rates of these modes are relatively insensitive to Mach number and are much larger than the growth rate of the center mode. They increase slightly in the very high Mach number regime. However, the growth rates are small compared to the growth rate of the center mode at low speeds. The outer modes should be the predominant instabilities at supersonic Mach numbers.

Next, consider the reacting flow ($T_{ad}=4$). As shown by Shin & Ferziger (1990) and others (Mahalingam *et al.* 1989), the low density created by reaction in the center of the shear layer reduces the growth rate of the center mode. Figure 2 shows that the growth rate of this mode is further reduced as the Mach number increases and is always smaller than the corresponding cold flow mode growth rate. As shown by Shin & Ferziger (1990), when T_{ad} is large enough, a set of outer modes arises in the reacting flow at low Mach numbers. For the case shown here, ($T_{ad}=4$), the outer modes are slightly less unstable than the center mode at $M_c=0$; this situation reverses at higher heat release. The growth rate of the outer modes falls off much more slowly with increasing Mach number, and for the heat release used here, they are the dominant modes for $M_c > 0.5$. At $M_c > 1$, there is a single pair of outer modes of the heated flow; they can be regarded as the extension of either the unheated supersonic flow or low-speed reacting flow reacting modes. Perhaps the most significant point to note is that the growth rate of the outer mode in the reacting supersonic flow is approximately twice that of the corresponding non-reacting flow. Thus, in contrast to the low speed case, heat release due to chemical

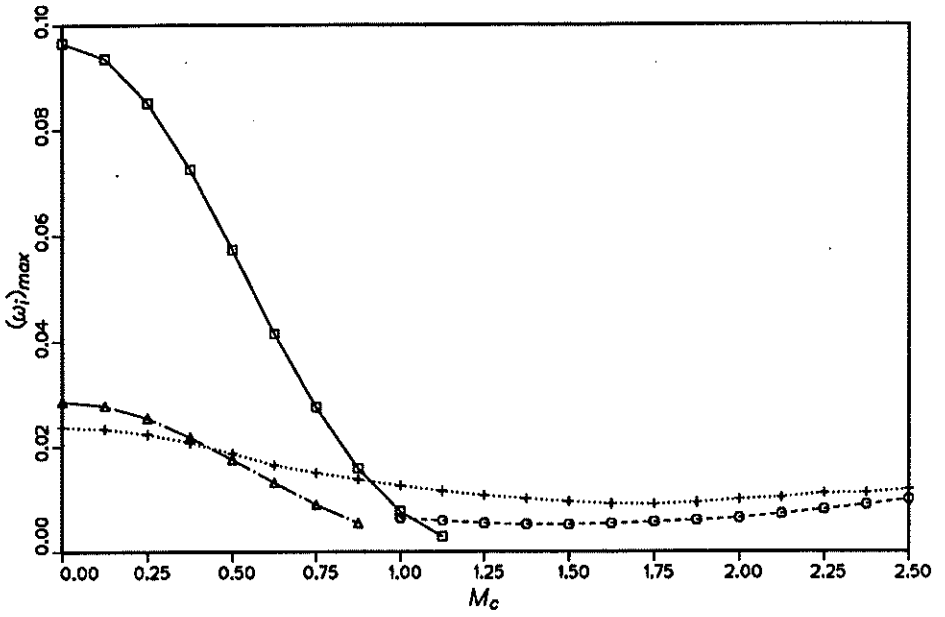

FIGURE 2. Maximum growth rate versus convective Mach number. □ , T_{ad}=1 (center mode); ○ , T_{ad}=1 (outer mode); △ , T_{ad}=4 (center mode); +, T_{ad}=4 (outer mode).

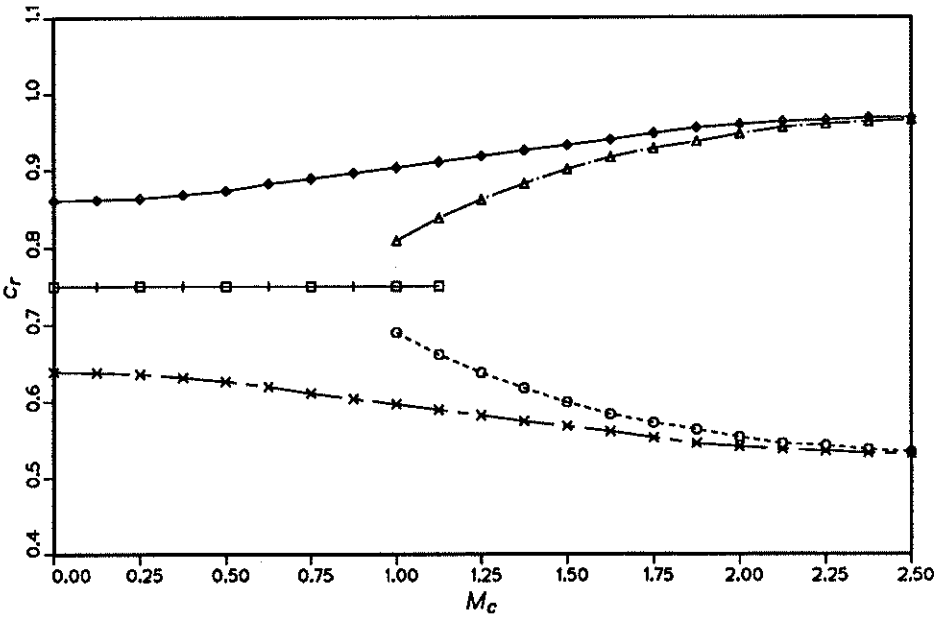

FIGURE 3. Phase speed corresponding Maximum growth rate versus convective Mach number. □ , T_{ad}=1 (center mode); ○ , T_{ad}=1 (slow mode); △ , T_{ad}=1 (fast mode); +, T_{ad}=4 (center mode); ×, T_{ad}=4 (slow mode); ◇ , T_{ad}=4 (fast mode).

reaction is destabilizing in supersonic flow. At higher heat release, these effects would be even larger. Again, the growth rates of the outer modes increase with increasing Mach number in the high Mach number regime.

Figure 3 gives the corresponding phase speeds. The center mode always travels at the average speed of two streams, whereas the fast mode travels faster than the average speed and the slow mode, slower. The phase speeds of the outer modes approach the free stream velocities as the Mach number increases. Increasing the adiabatic flame temperature raises the speed of the fast mode and reduces the speed of the slow mode in the outer modes at any Mach number. At very high Mach number, the speed of the outer modes becomes independent of the heat release.

We now study these modes in more detail. Figures 4-5 show the amplification rates and phase velocities as functions of wavenumber for convective Mach number 0.5 and 1.25, respectively. The corresponding upper-stream Mach numbers are 2 and 5 respectively. For M_c=0.5 and no reaction, only the center mode is unstable. As Mach number or heat release increases, the outer modes become unstable. The maximum growth rate of the outer modes at M_c=1.25 without reaction are only about one-tenth the maximum growth rate of the center mode at M_c=0.5 and T_{ad}=1; the wavenumber corresponding to maximum growth is half that at M_c=0.5. The T_{ad}=4, M_c=0.5 case has three distinct unstable modes, the center, fast, and slow modes. The amplification rate for this case has two maxima, one at α=0.15 due to the center mode and the other at α=0.58 due to the outer modes. The maximum growth rates of the two sets of modes are almost equal, but the other peak is much broader. The maximum growth rate is about one-third of the maximum for the corresponding case with zero heat release. Thus, heat release stabilizes the flow at M_c=0.5 and causes outer modes to appear. At M_c=1.25 and T_{ad}=4, as in the corresponding non-reacting flow, only the outer modes are unstable. The wavenumber is almost twice the non-reacting value, so heat release decreases the wavelength of maximum growth rate. The maximum growth rate is twice that of the T_{ad}=1 case, a trend opposite that found in the M_c=0.5 case.

Due to the symmetry of the mean profiles, the amplification rates of the two outer modes are the same, but the phase velocities are different. The phase velocity of the fast mode, which ranges from 0.8 to 0.9 at M_c=1.25 and T_{ad}=1, approaches the speed of upper stream as wavenumber increases, while that of slow mode approaches the speed of lower stream. At M_c=0.5 and T_{ad}=4, the phase speeds lie in the range of 0.75 to 0.92 for fast mode and 0.58 to 0.75 for slow mode. As the Mach number increases (M_c=1.25), the phase speed of the fast mode lies in the range of 0.81 to 0.95 and that of the slow mode in the range of 0.55 to 0.69.

2.4 Effect of heat release, variable properties, and reaction

In Section 2.1, we showed that heat release due to chemical reaction and the variation of properties through the reacting shear layer influence the mean flow profiles significantly. In this section, we study the effect of heat release, chemical reaction, and property variation on the stability of spatial layers. In the spatial case, the growth rates of the two outer modes are not equal. Figure 6 shows the effect of heat release on the maximum growth rate. At M_c=0.25 (M_1=1), as the

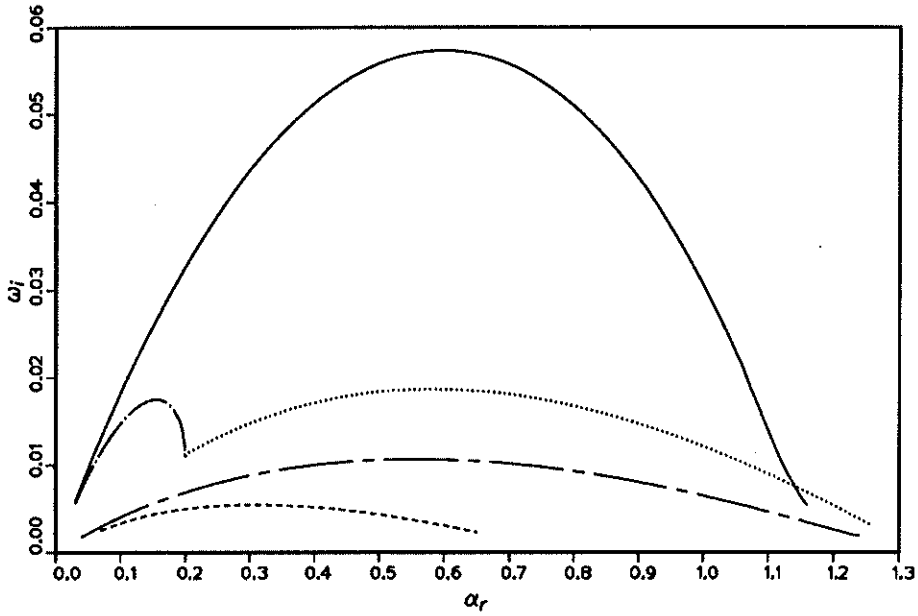

FIGURE 4. Growth rate versus wavenumber. ——— , T_{ad}=1 (M_c=0.5, center mode); - - - - , T_{ad}=1 (M_c=1.25, outer mode); —·— , T_{ad}=4 (M_c=0.5, center mode); ····· , T_{ad}=4 (M_c=0.5, outer mode); — — — , T_{ad}=4 (M_c=1.25, outer mode).

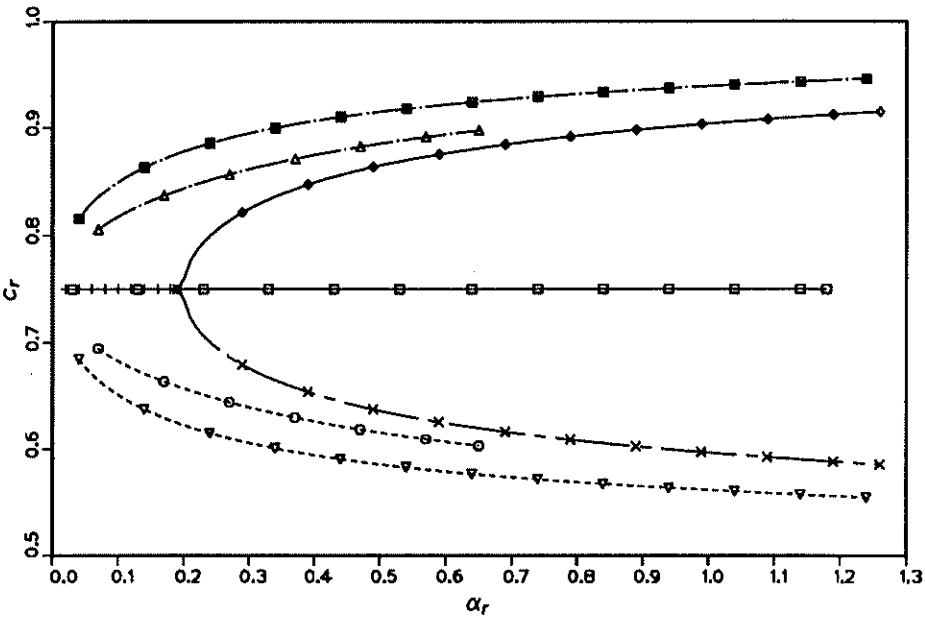

FIGURE 5. Phase speed versus wavenumber. □ , T_{ad}=1 (M_c=0.5, center mode); ○ , T_{ad}=1 (M_c=1.25, slow mode); △ , T_{ad}=1 (M_c=1.25, fast mode); +, T_{ad}=4 (M_c=0.5, center mode); ×, T_{ad}=4 (M_c=0.5, slow mode); ◇ , T_{ad}=4 (M_c=0.5, fast mode); ▽ , T_{ad}=4 (M_c=1.25, slow mode); ⊠ , T_{ad}=4 (M_c=1.25, fast mode).

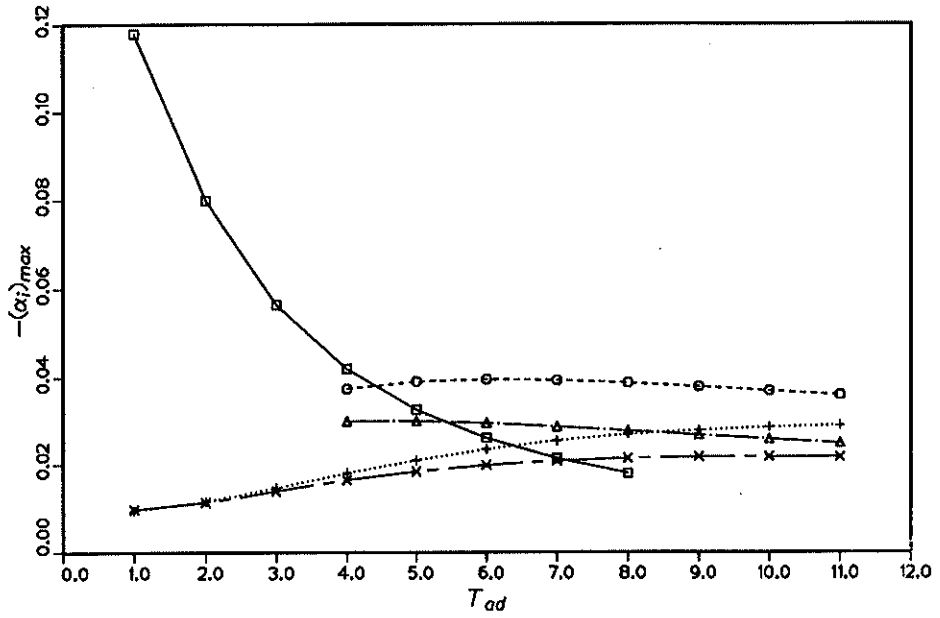

FIGURE 6. Maximum growth rate versus adiabatic flame temperature. □, M_c=0.25 (center mode); ○, M_c=0.25 (slow mode); △, M_c=0.25 (fast mode); +, M_c=1.25 (slow mode); ×, M_c=1.25 (fast mode).

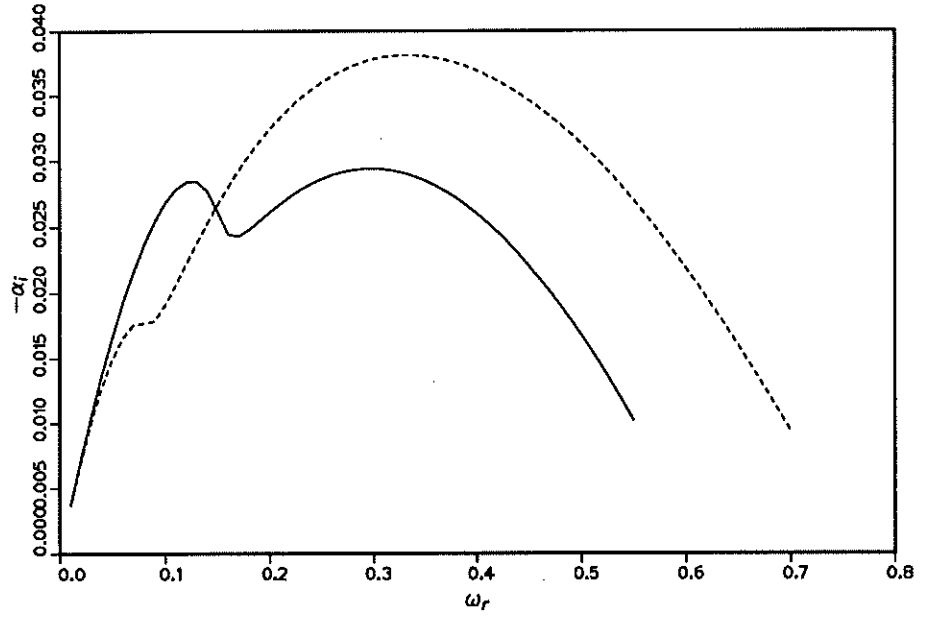

FIGURE 7. Effect of variation of properties on the growth rate at T_{ad}=8, M_c=0.25. ——, constant property; - - - -, variable property.

heat release increases, the maximum amplification rate of the center mode decreases rapidly. The maximum amplification rate in the cold flow is 0.118, while for T_{ad}=8 it is 0.018, or 15% the cold flow value. The amplification rates of the outer modes change very little as the heat release increases. The slow mode is more amplified than the fast mode. Consequently, at high heat release, the outer modes have larger amplification rates than the center mode, and the slow mode should dominate. For T_{ad}=8, the outer modes have almost twice the amplification rate of the center mode. Flows with high heat release should be unstable to the slow mode, but heat release stabilizes the flow at M_c=0.25 (M_1=1).

At M_c=1.25 (M_1=5), only the outer modes are unstable. As the heat release increases, the maximum growth rates increase. The maximum growth rate of slow mode for the non-reacting flow is 0.0095, while for T_{ad}=8 it is 0.027, or about three times as much. The fast mode grows more slowly than the slow mode, but at T_{ad}=11 it has twice the growth rate of most unstable mode in the non-reacting flow. Consequently, at high Mach number, the only outer modes are unstable and their growth rates increase with heat release.

Figure 7 shows the effect of variable properties on the stability characteristics when T_{ad}=8 and M_c=0.25 (M_1=1). The variable property center mode growth rate is two thirds the center mode growth rate of the constant property case; however, the maximum growth rate of the outer mode is almost 30% higher. The constant property profile gives center and outer modes with comparable amplification rates, but with the variable property profile, the outer modes dominate.

In low-speed flow, density variation in the laminar flow has a more significant effect than chemical reaction that occurs during the instability. Figure 8 shows that including the chemical reaction during the instability hardly changes the amplification rate in compressible flow. These results suggest that chemical reaction can be ignored in linear stability analysis.

2.5 Three-dimensional instability

In compressible flow, the obliquity of the most amplified wave increases as Mach number increases (Sandham & Reynolds 1989; Clemens & Mungal 1990). In this section, the effect of heat release on the obliquity of the most amplified mode is studied. Since maximum obliquity occurs at the high Mach number, we consider only the M_c=1.25 (M_1=5) case. Figure 9 shows the maximum amplification rates for various angles of propagation. In Figure 9, only the slow mode growth rates are plotted for readability; the fast modes have almost same growth rates. In a non-reacting mixing layer, for angles less than 30°, the outer modes are dominant and the maximum growth rates change little with angle. However, when the angle is greater than 40°, the outer modes disappear and the center mode begins to dominate. Its maximum amplification rate occurs at about 60° and is much greater than the growth rate of the outer modes at θ=0. Therefore, the most unstable mode is oblique at M_c=1.25. Clemens and Mungal (1990) reported that the flow is highly three-dimensional when $M_c > 0.6$, consistent with our predictions.

The reacting flow has very different behavior. At T_{ad}=2, the three modes behave as they do in the non-reacting flow but the center mode dominates only for angles

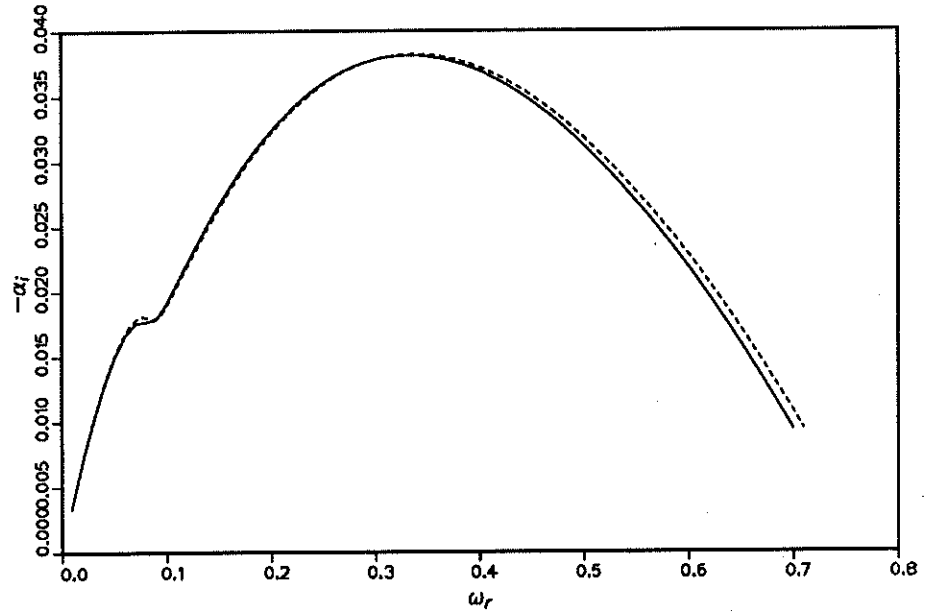

FIGURE 8. Effect of reaction during instability on the growth rate at T_{ad}=8, M_c=0.25. ——— , with chemical reaction; - - - - , without chemical reaction.

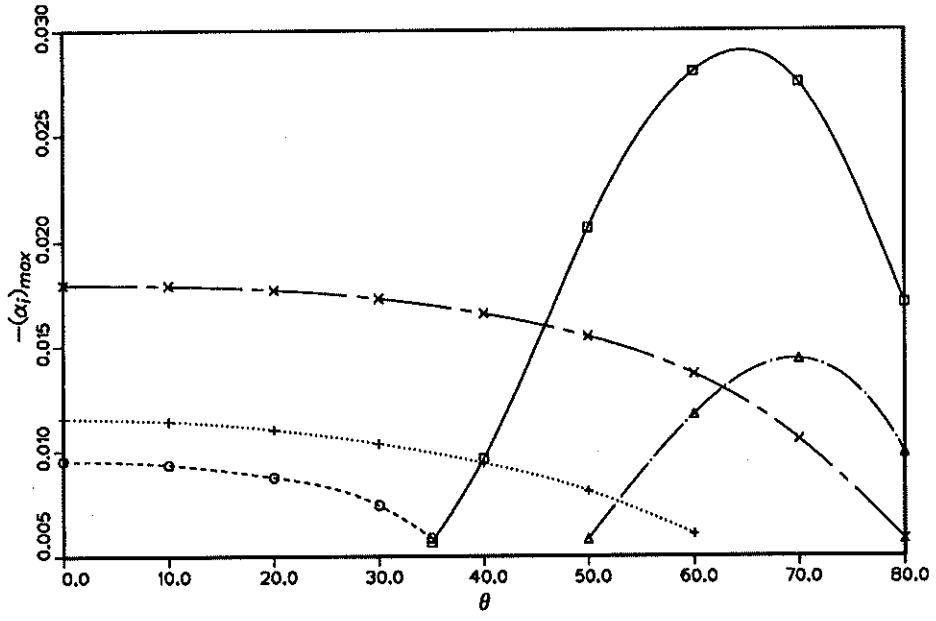

FIGURE 9. Maximum growth rate versus oblique angle at M_c=1.25. □ , T_{ad}=1 (center mode); ○ , T_{ad}=1 (slow mode); △ , T_{ad}=2 (center mode); +, T_{ad}=2 (slow mode); ×, T_{ad}=4 (slow mode).

above 55°; its maximum growth rate occurs at about 70°. As the heat release increases further (T_{ad}=4), the center mode disappears and only the outer modes are amplified. The maximum amplification rates of the outer modes decrease slightly as the obliquity increases. Therefore, heat release makes the dominant mode two-dimensional, even in the highly compressible regime. The three-dimensional modes which dominate in the non-reacting case are stable. In Section 2.4, we showed that the maximum amplification rate of the outer modes increases as heat release increases. For the conditions represented in Figure 9, the maximum amplification rate of the outer modes is about 1.4 times the rate in the non-reacting case. The phase velocities of outer modes approach the average velocity of the two streams as the angle increases.

3. Future plans

3.1 Effect of nonuniform density, stoichiometric ratio and finite chemistry

We have considered only the case of equal free stream densities. To be more realistic, we need to consider a flow in which the fuel and the oxidizer have different initial temperatures. We will study the characteristics of this flow and compare it with the uniform density flow. The stoichiometric ratio in the diffusion flame is defined by

$$\phi = \frac{(Y_F/Y_O)_{real}}{(Y_F/Y_O)_{ideal}} \tag{6}$$

where Y_F, Y_O represent the mass fractions of fuel and oxidizer, respectively. If $\phi > 1$, fuel is rich, while if $\phi < 1$ it is fuel lean. Changing ϕ changes mean flow profiles and the stability characteristics. We will look into this case. Finite rate chemistry is more realistic than the infinite rate chemistry of the flame sheet model. We will study the difference between two cases and establish the importance of using finite rate chemistry.

3.2 The effect of walls on a supersonic reacting mixing layer

Until now, we assumed the shear layers are free and unconfined. However, the situation is quite different in the supersonic mixing layers in a ramjet combustor. There is a coupling between the flow and acoustic modes through reflection of acoustic waves by the walls. This coupling will alter the stability of the shear layer. We will put the mixing layer in a channel to investigate this coupling. The mean flow will include chemical reaction. The stability equation will be derived. We will check the effects of all parameters such as heat release, Mach number, frequency, wavenumber, density ratio, stoichiometric ratio of fuel and oxidizer, thickness of shear layer, the height between walls and the direction of propagation of the disturbance wave. We will compare the results with and without walls. We hope this study will show the validity of using free shear flow.

Acknowledgements

The authors wish to acknowledge Mr. Olivier Planché for helpful discussions.

REFERENCES

BROWN, G. L. & ROSHKO, A. 1974 On density effects and large structure in turbulent mixing layers. *J. Fluid Mech.* **64**, 775–816.

BLUMEN, W., DRAZIN, P. G. & BILLINGS, D. F. 1975 Shear layer instability of an inviscid compressible fluid. Part 2. *J. Fluid Mech.* **71**, 305–316.

CLEMENS, N. T. & MUNGAL, M. G. 1990 Two- and three-dimensional effects in the supersonic mixing layer. *AIAA 90-1978.*

GROPPENGIESSER, H. 1970 Study on the stability of boundary layers in compressible fluids. *NASA TT-F-12.* rm **786**,

PAPAMOSCHOU, D. & ROSHKO, A. 1988 The compressible turbulent shear layer: an experimental study. *J. Fluid Mech.* **197**, 453–477.

SANDHAM, N. D. & REYNOLDS, W. C. 1989 A numerical investigation of the compressible mixing layer. Stanford University, Department of Mechanical Engineering, Thermosciences Division Report TF-45.

SHIN, D. S. & FERZIGER, J. H. 1990 Linear stability of the reacting mixing layer. *AIAA 90-0286.*